Permeability and Separation Characteristics of Polypeptide-Functionalized Polycarbonate Track-Etched Membranes

V. Smuleac,[†,‡] D. A. Butterfield,[‡] and D. Bhattacharyya*[,†]

Departments of Chemical and Materials Engineering, and Chemistry, University of Kentucky, Lexington, Kentucky 40506

Received December 15, 2003. Revised Manuscript Received May 10, 2004

The use of polypeptide-functionalized membranes with known porosity and uniform pore sizes allows a better understanding of the separation characteristics in nanodomains. A stimuli-responsive polypeptide, poly-L-glutamic acid (PLGA), was immobilized on a polycarbonate track-etched (PCTE) membrane. First, PCTE membrane was gold-coated under convective conditions, and a thiol, 3-mercapto 1,2-propanediol (MPD), was chemisorbed on the modified surface. Second, the MPD molecule was oxidized with sodium periodate to obtain an aldehyde functionality, which was further reacted with the amino group on the PLGA molecule, making possible a single point polypeptide attachment. The morphology of the modified membrane was analyzed by electron microscopy (SEM, TEM) imaging, confirming uniform structure. Modified membrane performances, with starting diameters of 30 and 100 nm, were evaluated in terms of solute (ionic and neutral) rejections and water permeability. Both solute and water transport through membrane were reversibly regulated by pH. The effective membrane charge was calculated using the extended Nernst−Plank equation coupled with Donnan equilibrium and electroneutrality conditions.

1. Introduction

The chemical modification and functionalization of polymeric materials is of great interest in separation science.[1,2] The immobilization of appropriate functional groups inside membrane pores allows selective transport of solute species. Biomolecules such as polypeptides, which undergo conformational changes in response to an external stimuli such as pH, ionic strength, or temperature, are useful for achieving controlled flux and separations. Various studies on polypeptide immobilization on membrane surfaces and their application and physical properties have been reported in the literature: chiral separations,[3] heavy metal capture,[4,5] tunable membranes[6] and in gel-filled membranes,[7,8] and the influence of polypeptide conformational changes on membrane properties.[9−12]

Polycarbonate track-etched membranes are excellent supports because of their uniform pore geometry and narrow pore size distribution, and these membranes can be considered a model system for studying selective separation behavior. The electroless gold plating method followed by thiol chemisorption has been used for the modification of polycarbonate membranes.[12,13] A large number of molecules can be immobilized via the thiol linkage, thereby modifying the membrane surface with various functional groups.

Applications of thiol−gold chemistry include catalysis, sensing, and separations. In the field of separations, gold-coated membranes functionalized with thiols were used in modulating the transport of species based on hydrophobic/hydrophilic interactions,[13,14] ion-selectivity via ionizable thiols[15−17] and applied potential.[18−20] Polycarbonate membranes also have been used as a templates to produce size-controlled self-assembly of polypeptide nanotubules or nanotube-templated metallized wires, with potential applications in electronics and sensors.[21,22]

* Corresponding author. Phone: 859-257-2794. Fax: 859-323-1929. E-mail: db@engr.uky.edu.
[†] Department of Chemical and Materials Engineering.
[‡] Department of Chemistry.

(1) *New Insights into Membrane Science and Technology: Polymeric and Biofunctional Membranes*; Bhattacharyya, D., Butterfield, D. A., Eds.; Elsevier: Amsterdam 2003.
(2) *Polymeric Ligand-Based Functionalized Materials and Membranes for Ion Exchange;* Ritchie, S. M. C., Bhattacharyya, D., Eds.; Marcel Dekker: New York, 2000; pp 81−118.
(3) Lee, N. H.; Frank, C. W. *Polymer* **2002**, *43*, 6255−6262.
(4) Bhattacharyya, D.; Hestekin, J. A.; Brushaber, P.; Cullen, L.; Bachas L. G.; Sikdar, S. K. *J. Membr. Sci.* **1998**, *141*, 121−135.
(5) Ritchie, S. M. C.; Bachas, L. G.; Olin, T.; Sikdar, S. K.; Bhattacharyya, D. *Langmuir* **1999**, *15*, 6346−6357.
(6) Hollman, A. M.; Bhattacharyya, D. *Langmuir* **2002**, *18*, 5946−6002.
(7) Mika, A. M.; Childs, R. F. *Ind. Eng. Chem. Res.* **2003**, *42*, 3111−3117.
(8) Mika, A. M.; Childs, R. F.; Dixon J. M. *J. Membr. Sci.* **2002**, *206*, 19−30.
(9) Ito, Y.; Ochiai, Y.; Park, Y. S.; Imanishi, Y. *J. Am. Chem. Soc.* **1997**, *119*, 1619−1623.
(10) Ito, Y.; Park, Y. S.; Imanishi, Y. *Langmuir* **2000**, *16*, 5376−5381.
(11) Zhang, H.; Ito, Y. *Langmuir* **2001**, *17*, 8336−8340.
(12) Ito, Y. *J. Am. Chem. Soc.* **1997**, *119*, 2739−2740.
(13) Hulteen, J. C.; Jirage, K. B.; Martin, C. R. *J. Am. Chem. Soc.* **1998**, *120*, 6603−6604.
(14) Jirage, K. B.; Martin, C. R. *Anal. Chem.* **1999**, *71*, 4913−4918.
(15) Hou, Z.; Abbott, N. L.; Stroeve, P. *Langmuir* **2000**, *16*, 2401−2404.
(16) Chun, K. Y.; Stroeve, P. *Langmuir* **2002**, *18*, 4653−4658.
(17) Lee, S. B.; Martin, C. R. *Anal. Chem.* **2001**, *73*, 768−775.
(18) Lee, S. B.; Martin, C. R. *Chem. Mater.* **2001**, *13*, 3236−3244.
(19) Chun, K. Y.; Stroeve, P. *Langmuir* **2001**, *17*, 5271−5275.
(20) Kang, M. S.; Martin, C. R. *Langmuir* **2001**, *17*, 2753−2759.

10.1021/cm035323j CCC: $27.50
Published on Web 06/16/2004

The template method, originally proposed by Martin and co-workers,[17,23] has led to the development of novel membrane architectures. The objectives of the current research included (1) modification of the electroless plating technique to maintain the defined pore structure of the host material, (2) development of a new method of immobilizing a polypeptide on a membrane with a defined structure, and (3) evaluation of the membrane performance in terms of permeability and retention capacity of charged inorganic species and neutral organic solutes. The effects of various parameters, such as pH, feed concentration, solute charge, membrane pore size, polypeptide chain length, and permeate flux, on the membrane performance were investigated. The effective membrane charge was calculated from a simplified model derived from the extended Nernst−Plank equation. This paper reports the results of these studies.

2. Experimental Section

2.1. Electroless Gold Plating. Poly(vinylpyrrolidone) (PVP)-coated track-etch polycarbonate (PCTE) membranes with pore diameters from 30 to 400 nm (membrane thickness 6−10 μm) were used in these experiments and were obtained from Osmonics. $AgNO_3$, $NaHCO_3$, and Na_2SO_3 were purchased from JT Baker; $SnCl_2$ was obtained from Aldrich; and CF_3COOH and formaldehyde were purchased from Mallinckrodt. The gold plating solution, Oromerse SO Part B, was obtained from Technic, Inc.

PCTE membranes were coated with a thin layer of gold, using an electroless gold-plating method. We modified the procedure found in the literature,[14] performing the plating under convective flow in a pressurized filtration cell, instead of diffusive conditions This modification allowed deposition of a uniform layer of gold on the membrane pore walls.

The filtration cell used, Sepa ST (dead-end), was obtained from Osmonics. The cell was used for gold plating, steps following membrane functionalization, and solute permeation studies. This magnetically stirred cell reduced the concentration polarization. Depending on the membrane, transmembrane pressures from 10 to 14 bar (for the 30 nm membrane) and 0.5 to 2 bar (for the 100 nm membrane) were used. A typical procedure consisted of (i) Sn^{2+} coating on the PVP layer of the membrane; (ii) Ag deposition; and (iii) displacement of Ag by Au. After the gold plating, the membranes were immersed in 25% HNO_3 aqueous solution for 12 h, to remove residual Sn and Ag from the membrane. Gold-coated membranes were analyzed by SEM and TEM imaging. The surface for bare and gold-coated membranes (using N_2 at 77 K) was determined using a Micromeritics ASAP 2000 surface area analyzer.

To quantify the amount of gold deposited on the membrane, the feed and permeate concentration of Au was measured by atomic absorption spectroscopy, and the difference was assumed to be the amount of gold adsorbed on the membrane. The analytical error for Au analysis in the range 2.5−20 mg/L was <2.5%.

2.2. Membrane Functionalization. All chemicals were purchased from Sigma, unless otherwise stated. Using the established affinity of thiols for gold, 3-mercapto-1,2-propanediol (MPD) was chemisorbed on the gold-modified membrane surface. Typically, 100 mL of 0.5 mM MPD was permeated through the membrane, followed by the oxidation of the diol functionality to aldehyde using 23 mM $NaIO_4$. Then, using the Schiff base reaction, poly-L-glutamic acid (PLGA) was immobilized on the membrane by reacting the terminal amine on the polypeptide with the aldehyde group on the membrane surface. The imine bond formed was reduced to a secondary amine, by $NaBH_4$, to enhance broad pH stability. All functionalization reactions were carried out in a stirred ultrafiltration cell under pressure. A schematic drawing of membrane functionalization employed in these studies is given in Figure 1.

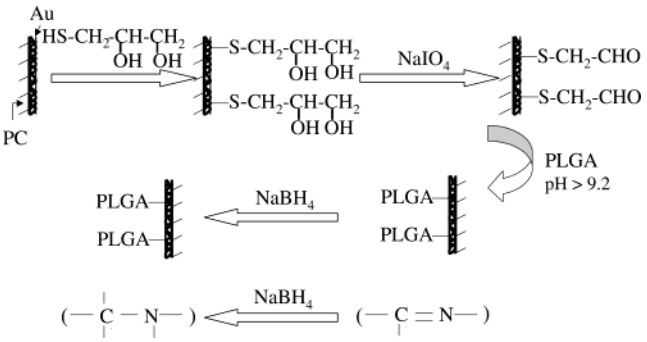

Figure 1. Gold-modified polycarbonate track-etched (PCTE) membrane functionalization.

PLGA molecules of 17 500 MW (116 repeating units) were immobilized on the 30 nm PCTE membrane, and PLGA molecules of 54 000 MW (356 repeating units) were immobilized on the 100 nm PCTE membrane. The amount of PLGA immobilized on each membrane was estimated by two methods. First, from Cd^{2+} ion exchange, i.e., we monitored the concentration of Cd^{2+} in the permeate, using a Varian SpectAA220 FS atomic absorption spectrometer and assuming that 1 mol Cd^{2+} binds 2 mol of COO^- groups. Three replicates were taken for each measurement, and the errors were <1.5%. The second method used was total organic carbon analysis, for feed and permeate, using a TOC-5000A Shimadzu analyzer. Also three replicates were taken for each measurement, and the error was <3%. The results from both methods were in good agreement.

The amount of MPD immobilized on the membrane was estimated using a procedure introduced by Ellman,[24] based on the absorbance at 412 nm of the 2-nitro 5-thiobenzoate ion at pH 8, produced from the reaction of 5,5′-dithiobis(2-nitrobenzoic acid) (DTNB) with the thiol groups. Because we used $NaIO_4$ in excess (typically 1−2 g/L), we assumed that all diol functionalities from MPD molecules were oxidized to aldehyde making the ratio of mmol MPD chemisorbed/mmol aldehyde equal to 1. On the basis of this assumption, we can estimate the polypeptide attachment efficiency, defined as the percentage of the available aldehyde groups that react with terminal amine of the polypeptide.

2.3. Analysis of Membrane Performance. Membrane performance was analyzed in terms of water permeability and salt and organic separations. After polypeptide immobilization, a decrease in permeability and its strong dependence on pH of the feed solution confirmed the presence of polypeptide on the membrane.

The membrane performance was extensively evaluated in terms of separation of ionized (NaCl and Na_2SO_4) and neutral organic (poly(ethylene glycol), dextran) solutes, defined as

$$R = \left(1 - \frac{C_p}{C_f}\right)100 \qquad (1)$$

where R is the solute rejection and C_p and C_f are the concentrations of the permeate and feed solutions, respectively. Diluted inorganic salt solutions in the range of 0.2−5 mM were used to test the separation capabilities of the functionalized membranes. The salt concentration in the feed and permeate solutions was measured (Na^+ analysis) by atomic absorption spectroscopy. The rejection of neutral organic molecules was performed in order to estimate the molecular weight cutoff of

(21) Porrata, P.; Goun, E.; Matsui, H. *Chem. Mater.* **2002**, *14*, 4378−4381.
(22) Matsui, H.; Pan, S.; Gologan, B.; Jonas, S. H. *J. Phys. Chem. B* **2000**, *104*, 9576−9579.
(23) Menon, V. P.; Martin, C. R. *Anal. Chem.* **1995**, *67*, 1920−1928.
(24) Ellman, G. L. *Arch. Biochem. Biophys.* **1959**, *82*, 70−75.

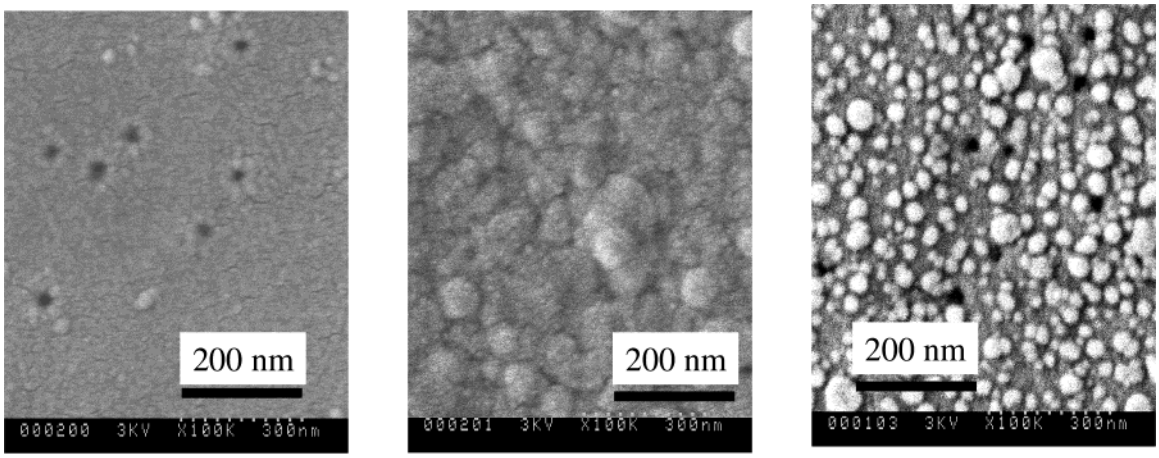

Figure 2. SEM (100 000×) images for the 30 nm polycarbonate membranes: (a) bare (uncoated) membrane; (b) gold-coated membrane, plating performed under static conditions; (c) gold-coated membrane, plating performed under convective flow (maintaining a flux of 3.3×10^{-4} cm^3/cm^2 s).

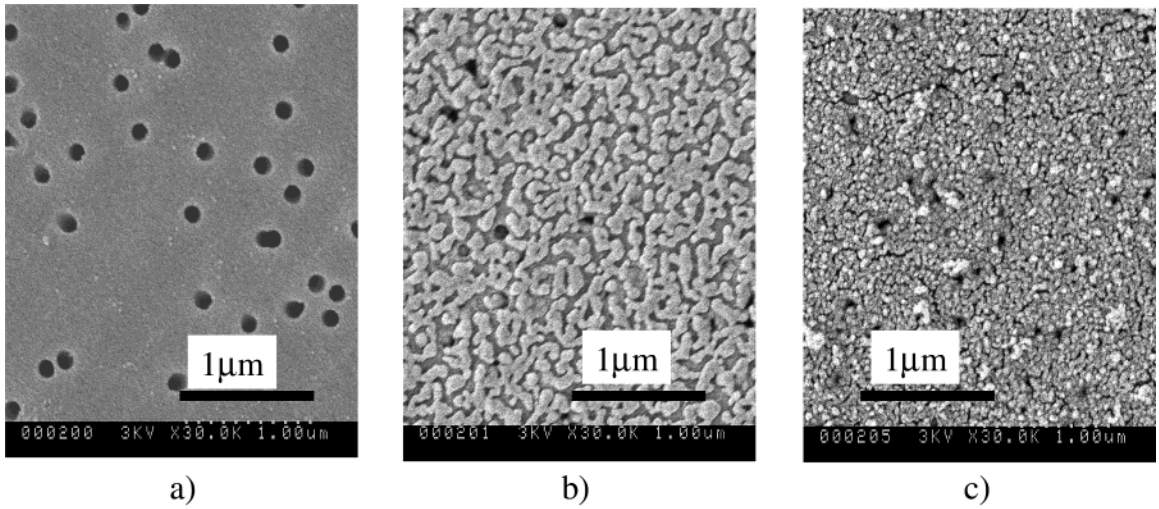

Figure 3. SEM images for the 100 nm PCTE membrane (30 000×): (a) bare membrane; (b) Au-coated, plating performed under static conditions; (c) gold-coated, plating performed under convective flow (maintaining a flux of 8.9×10^{-4} cm^3/cm^2 s).

the modified membrane. The concentration of organic molecules in the feed and permeate solutions was measured by a total organic carbon analyzer (TOC). The experimental error for Na^+ analysis was about 0.2−1.2%, and the error for TOC was about 1−4%.

3. Results and Discussion

3.1. Electroless Gold Plating. The electroless gold plating was performed using two methods: under diffusive conditions (immersing the membrane in a plating bath), as well as using convective flow (when the membrane was mounted in a filtration cell and the plating solution was permeated through the membrane). These two methods were compared as noted below.

When gold plating was performed under diffusive conditions, gold preferentially deposits on the membrane surface, forming aggregates. This formation of "bottleneck pores" was reported previously.[15,23] These aggregates covered a substantial number of pores, lowering the membrane porosity. This aggregation was observed by comparing SEM images for membrane surfaces that are unmodified (Figures 2a, 3a, and 4a) and gold-plated under static conditions (Figures 2b, 3b, and 4b).

To minimize the preferential deposition of gold on the membrane surface and formation of aggregates and also to stimulate gold deposition on the pore walls, we performed the gold plating in a stirred filtration cell, loading the plating solution in the feed and passing it through the membrane at low permeation rates. SEM images of the gold-plated membrane surface under convective conditions (Figures 2c, 3c, and 4c) show the formation of small particles instead of aggregates. During plating the pressure had to be increased in order to maintain the flux, which dropped due to gold deposition. Thus, for the 30 nm membrane, the pressure was increased from 2 to 4 bar, for a flux of 3.3×10^{-4} cm^3/cm^2 s. For the 100 nm membrane, the pressure was increased from 0.1 to 0.3 bar, the flux being 8.9×10^{-4} cm^3/cm^2 s.

A more dramatic decrease in porosity that results when the gold plating takes place under static instead of convective conditions was observed from pure water flux measurements. Under the same plating conditions (same Au feed concentration in the plating bath and the same plating time), for a membrane with very open structure (400 nm pore diameter), the flux decrease

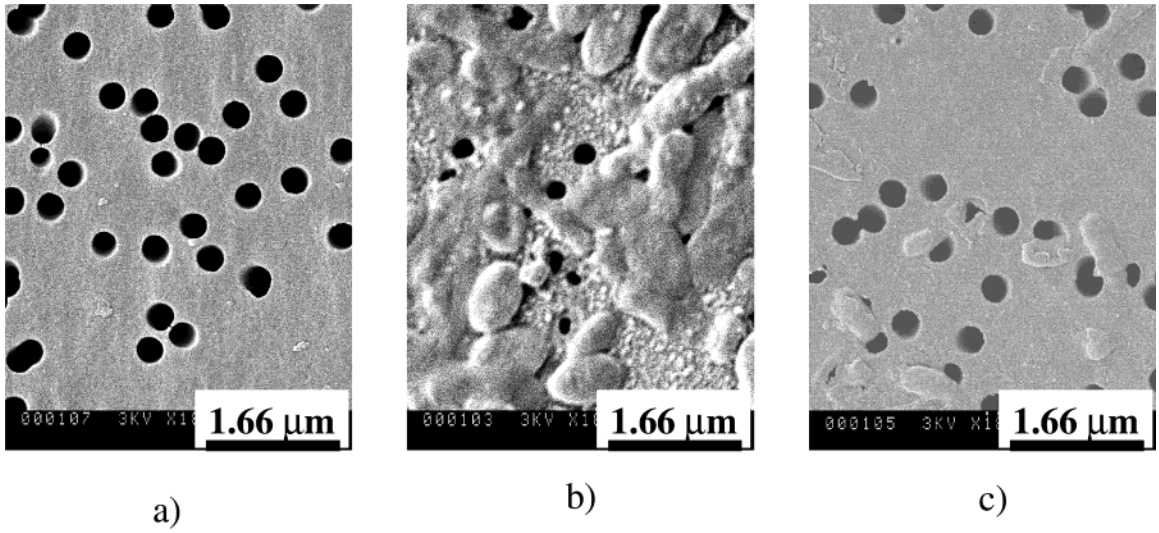

Figure 4. SEM (18 000×) images of the 400 nm polycarbonate membranes: (a) bare (uncoated) membrane; (b) gold-coated membrane, plating performed under static conditions; (c) gold-coated membrane, plating performed under convective flow (maintaining a flux of 23×10^{-4} cm^3/cm^2 s).

after diffusive plating was 50%, whereas under convective plating the flux drop is <20%.

Figure 5 shows the cross section for the gold-coated 100 nm membrane (top) and the EDS (energy dispersive spectroscopy) spectrum (bottom), confirming the presence of gold. Gold plating takes place on both membrane surfaces as well as on the membrane pore walls. However, the coating is not continuous throughout the pore; the reason for this may be that the membrane was not uniformly coated with (PVP). PCTE is coated by the manufacturer (Osmonics) with PVP in order to make the membrane hydrophilic, and it is necessary in the first step of elelctroless plating;[14,23] without PVP no coating takes place.

3.2. Membrane Functionalization. After gold plating, the membrane was functionalized with a polypeptide, as described above. PLGA ($pK_a = 4.38$) is a molecule that undergoes conformational changes as a function of pH; at low pH (<5.5), PLGA is in a helix conformation, in which the polymer chains shorten and the carboxylic acid groups remain uncharged. At pH >5.5 the polyamino acid is in a random coil conformation, in which the chains are extended and the carboxylic acid groups are charged.[4,6,9] We predict that membrane performance (permeability, charged solute rejections) will be different at pHs below and above the pK_a. The length of one repeat unit is 0.35 nm for the random coil and 0.15 nm for the helix conformation.[6] When PLGA with 116 and 356 repeat units is immobilized on membranes with 30 and 100 nm pore diameter, respectively, the ratio of PLGA chain length (assuming chains are 90% extended) and membrane pore size approaches 1 for both the low and high MW polyamino acids and membranes used. Polymer chains will not cover the entire pore volume, and there also will be gaps between chains. The size of the pore region not covered by chains has a major effect on the membrane performance (see below).

3.3. Attachment Efficiency. The amount of MPD chemisorbed on gold-coated membranes was estimated from the reaction with DTNB, as mentioned above. The total amount of MPD immobilized in a membrane of 13.2 cm^2 surface area was estimated to be 1.16×10^{-2} mmol, calculated by subtracting the amount of thiol in the permeate and wash from the initial amount in the feed. This is the maximum amount of polypeptide that can be immobilized on the membrane; however it is expected that MPD, due to its small size (FW ~ 119), will have much higher chain density than PLGA (17 500 or 54 000 MW).

The total amount of 17 500 MW PLGA immobilized on several 30 nm pore size membranes was estimated to be in the range from 3×10^{-5} to 1×10^{-4} mmol at the highest loading. We can calculate the amount of polypeptide immobilized per unit membrane area, if we divide the total amount by the total membrane area (A_t), calculated by adding the surface A_s (13.2 cm^2) and internal pore areas: $A_t = A_s(1 - \theta) + (2\pi r_p L)\sigma A_s$, where θ, σ, r_p, L are membrane porosity, pore density, pore radius, and membrane thickness, respectively.

For example, the total area for the 30 nm pore diameter gold-coated membrane, assuming a straight cylindrical pore, values for porosity ($\theta = 0.47\%$) and average pore radius ($r_p = 12.2$ nm) from SEM images, and manufacturer's data for membrane thickness $L = 6$ μm and pore density $\rho = 6 \times 10^8$ pores/cm^2, is 74.2 cm^2. Thus, the loading would correspond to 1.6×10^{-4} mmol/cm^2 for MPD and from 4.8×10^{-7} to 1.7×10^{-6} mmol/cm^2 for 17 500 MW PLGA attached on the 30 nm membrane. For the 100 nm membranes immobilized with 54 000 MW PLGA, the total area calculated in the same way is 115 cm^2, respectively, and the amount of polypeptide attached per unit area is 6.3×10^{-8} and 1.25×10^{-6} mmol/cm^2, for the two different membranes.

However, it should be noted that the total surface area was calculated by assuming that the pores are cylindrical and the surface after gold coating is flat. However, as can be observed from SEM images, the membrane is covered by a multitude of particles 20−30 nm in diameter, which will increase the total surface area. Also, microscopic investigations[22] have shown that the pores are not cylindrical but "cigarlike", the pore inside the membrane being wider than on the surface by a factor of 3. These irregularities can explain the discrep-

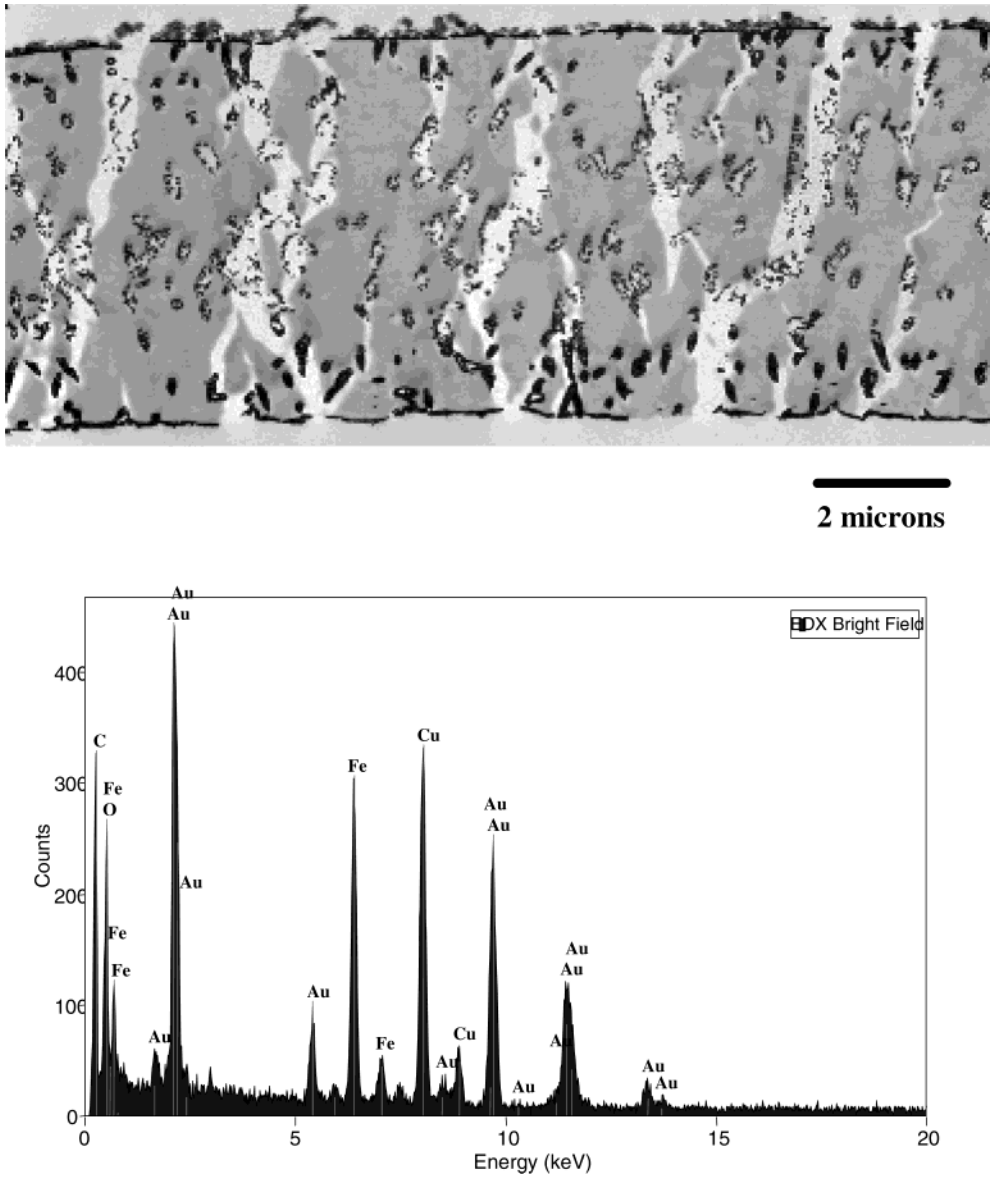

Figure 5. TEM (6800×) (top) and EDS of the cross section of gold-coated 100 nm PCTE (bottom).

ancies between the measured total area, from BET, and the calculated one, as explained above. Thus, from BET, the area was determined to be 1.96 m^2/g for bare and 5.54 m^2/g for gold-coated membranes. Knowing the weight for each membrane (0.0120 and 0.0199 g, respectively), this would correspond to a total area of 178.6 cm^2 for bare and 839.8 cm^2 for the gold-coated membrane, which are respectively 3 and 10 times higher than the calculated area using manufacturer's data and SEM images. Nevertheless, it can be observed that even at the highest loading, the attachment efficiency does not exceed 1% of the available aldehyde groups. The reason for this relatively low degree of attachment will be explained in following sections.

3.4. Molecular Weight Cutoff (MWCO) Analysis. Neutral organic solute rejection was performed to determine the molecular weight cutoff of the membrane. The pH of the feed solution was kept above 6 to keep the polypeptide chains extended, thus allowing the estimation of the size of the pore region not occupied by polypeptide chains. When the rejection was analyzed as a function of molecular size of neutral organics (estimated from the correlations found in the literature[25,26]) for the 30 nm membrane immobilized with 17 500 MW PLGA, we observed a steep increase in rejection for molecules with an average diameter in the range of 4.5−4.7 nm. However, after increasing the size of the organic molecules to be rejected even to 15 nm, the rejection still did not reach 90% (Figure 6). This was attributed to the fact that organic molecules [poly(ethylene glycol)] (PEG) have a polydispersity of more than 1.15, which will cause the molecules of smaller size to pass through the membrane, giving an apparent rejection lower than in fact occurs. In the case of dextran, the polydispersity is more than 2, giving an erroneous estimation of the MWCO. To eliminate particles of lower molecular weight, the diafiltration technique was used. Since the rejection of neutral organics is only based on steric effects, we assumed that smaller molecules will pass through the membrane first. Under

(25) Reber, N.; Spohr, R.; Wolf, A.; Omichi, H.; Tamada, M.; Yoshida, M. *J. Membr. Sci.* **1998**, *140*, 275−281.
(26) Lindau, J.; Jonsson, A. S.; Bottino, A. *J. Membr. Sci.* **1998**, *149*, 11−20.

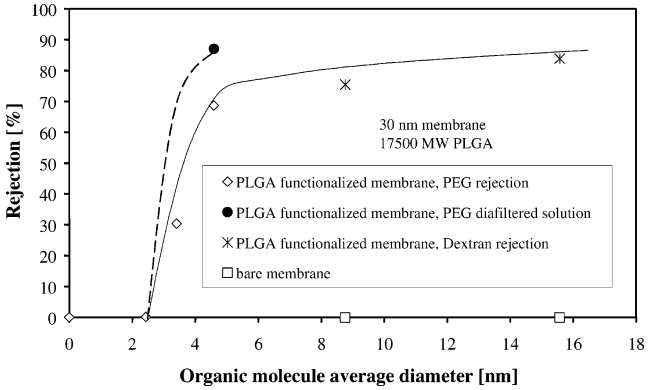

Figure 6. The rejection of PEG and dextran of known dimensions by 30 nm membranes.

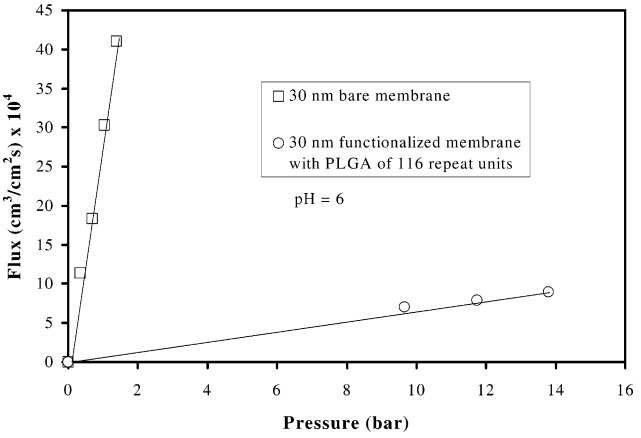

Figure 7. Water flux dependence on pressure for 30 nm PCTE membranes.

standard operating conditions, we started with 100 mL of a 500 mg/L (expressed as carbon) solution. After passing about 60 mL through the membrane, 60 mL of water was added. This step was repeated two more times, until the feed solution was about 100 mg/L. After this treatment, the rejection studies were performed with the diafiltered solution with the assumption of a much lower molecular size distribution. Consistent with this assumption, the rejection indeed increased by over 20%. The dashed line in Figure 6 represents the real rejection of standard organics, compared to the apparent one that is caused by dextran and PEG polydispersity. It is expected that these large neutral solutes will escape mainly through the central region of the pore, not covered by polymer chains. The formation of a transient gap between chains is unlikely to take place, due to the fact that the neutral solute rejection was conducted at low permeation rates (5.6×10^{-4} cm^3/cm^2 s), and the polypeptide chain density is high; as a consequence, the chain mobility will be minimized. On the basis of this type of analysis, the size of the pore region not occupied by polymer chains was estimated to be about 4.6 nm for the 30 nm membrane immobilized with 17 500 MW PLGA, and 37.6 nm for the 100 nm pore size membrane immobilized with 54 000 MW PLGA.

Pore diameters for bare, gold-coated, and PLGA-modified membranes were also determined from pure water flux measurements. There is a linear dependence of flux on applied pressure for bare and PLGA-modified 30 and 100 nm membranes, as can be seen in Figures 7 and 8. Typical permeabilities for bare and functionalized

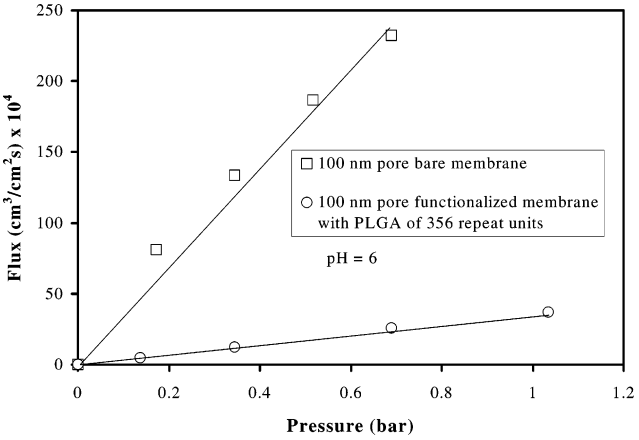

Figure 8. Water flux dependence on pressure for 100 nm PCTE membranes.

Table 1. PCTE Membrane Water Permeabilities (pH 6) after Various Steps of Functionalization

	L_p[a] (cm^3/cm^3 s bar)	
membrane	30 nm membrane	100 nm membrane
bare membrane	8.1	80.6
after gold coating	1.3	11.1
after MPD functionalization	1.3	11.1
after PLGA functionalization	0.1[b]	6.1[c]

[a] L_p = water permeability (flux/(thickness)(bar)). [b] Functionalized with PLGA of 116 repeat units (MW = 17 500). [c] Functionalized with PLGA of 356 repeat units (MW = 54 000).

membranes are presented in Table 1. As expected, there is a significant permeability drop after gold coating, but MPD chemisorption did not cause a detectable change in permeability. After PLGA attachment, there is a 10-fold reduction in permeability for the 30 nm pore size membrane, whereas for the 100 nm membrane, the permeability is only 2-fold lower after PLGA immobilization. Lower permeability is due to the fact that most of the pore volume is occupied by polypeptide chains.

Applying the Hagen−Poisseuille law of capillary flow (eq 2), assuming straight cylindrical pores and using the manufacturer's data for thickness (L) and pore density (σ), we estimated the pore size of each type of membrane, bare, after gold coating, and after functionalization (the gap between chains),

$$d = 2\left(\frac{8Q\mu L}{\pi \Delta P A \sigma}\right)^{1/4} \qquad (2)$$

where Q is water flow rate, μ is water viscosity, A is membrane surface area, and ΔP is transmembrane pressure. The calculated diameters resemble the results obtained from rejection of neutral organics only qualitatively; there is a discrepancy between nominal pore diameters provided by the manufacturer for bare membranes of 30 and 100 nm and the diameters calculated from the Hagen−Poisseuille law: 60 and 112 nm, respectively (Table 2). The discrepancy is more significant for smaller pore size membrane, when higher pressure has to be applied. This may be attributed to the flexibility of the polycarbonate membrane (pores expand due to stress), but no evidence of membrane tearing can be observed from SEM imaging. Similar disparities, when the pore diameter calculated using the Hagen−Poisseuille equation was between 2 and 4 times

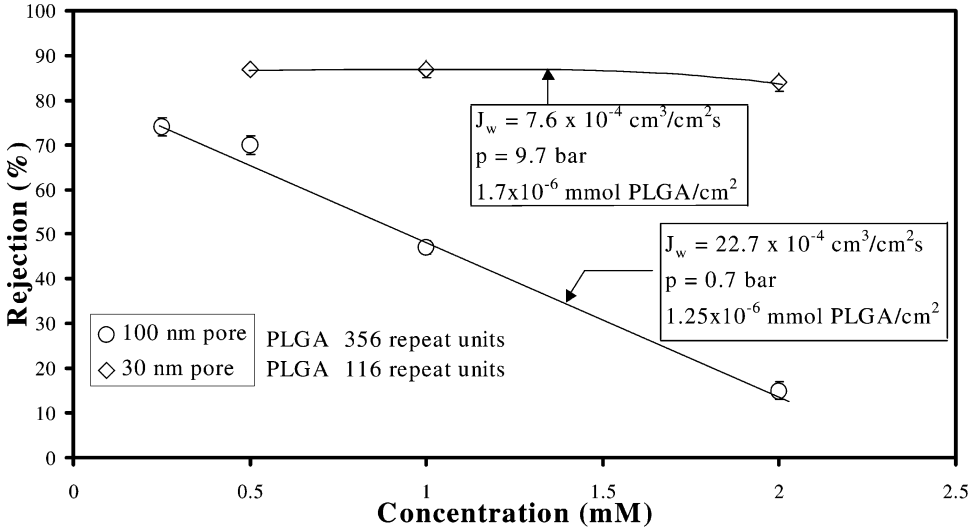

Figure 9. The influence of the Na_2SO_4 feed concentration on rejection.

Table 2. Calculated Pore Diameters Using the Hagen−Poisseuille Equation

membrane	30 nm	100 nm
bare membrane	60	113
after gold coating	43	74
after PLGA functionalization	24[a]	64[b]

[a] Functionalized with PLGA of 116 repeat units (MW = 17 500). [b] Functionalized with PLGA of 356 repeat units (MW = 54 000).

higher than the nominal pore diameter, were reported previously.[15,27]

3.5. Charged Solute (Salts) Rejection Studies. To establish the separation capabilities of the functionalized membranes, dilute inorganic salts were passed through the membrane and the influence of various parameters on rejection, such as solute charge and feed concentration, the amount of PLGA immobilized, flux (pressure), and pH, were investigated. Since the separation of salts is based on the Donnan exclusion mechanism for co-ions, the above parameters are strongly dependent on effective membrane charge. A calculation was performed in order to estimate the membrane charge at the highest polypeptide loading, using the extended Nernst−Planck equation coupled with the Donnan equilibrium and neutrality conditions.

3.5.1. Influence of Anion Charge and Feed Concentration. According to the ion exclusion theory by an electric field (the Donnan effect), in a charged membrane in contact with an electrolyte solution the concentration of the co-ions will be lower in the membrane than in the solution, whereas the counterion concentration in the membrane will be higher than in the solution. Thus, for a negatively charged membrane, the rejection of sulfate ion (2−) will be higher than that for chloride ion (1−), due to higher membrane−anion repulsion. The rejection ratio SO_4^{2-}/Cl^- increased from 2 to 4 with increasing feed concentration of Na_2SO_4 and NaCl from 0.5 to 2 mM.

The salt rejections decrease as the electrolyte concentration increases (Figure 9). This is due to the shielding effect of the cations on the membrane's negatively charged groups becomeing stronger as concentration increases, leading to the decrease of the membrane repulsion forces on the anions. This effect is more evident for monovalent anions (chloride) than for divalent anions (sulfate), the former having a higher charge density. The different behavior shown by the 30 and 100 nm membranes was attributed to different degrees of PLGA attachment and leakage effects, which are going to be discussed below.

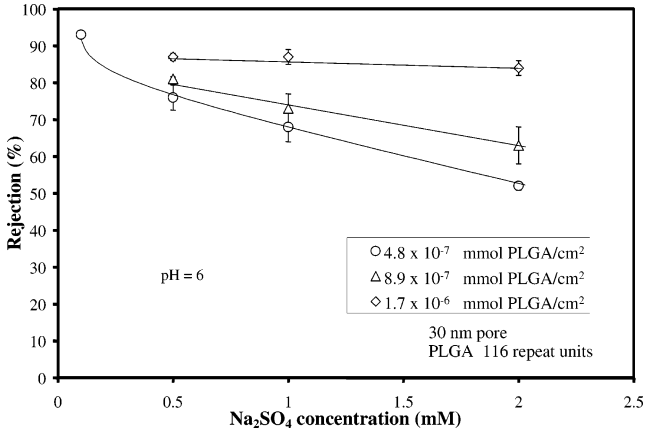

Figure 10. The influence of the amount of PLGA immobilized on the membrane on rejection capacity.

An interesting aspect regarding membrane separations capabilities is their long-term stability. For example, for the 30 nm membrane immobilized with 17 500 MW PLGA, after 1.5 months of operation, Na_2SO_4 (2 mM feed solution) rejection decreased only by 5%, from 84% to 80%.

3.5.2. Influence of the Amount of PLGA Immobilized on the Membrane. The total membrane charge is directly related to the density of charged polypeptide chains (amount immobilized); consequently, the membrane with a higher charge density will show higher rejection, as mentioned above. At dilute solute feed concentration there is a small difference among retention capabilities that is due to leakage through the pore area not covered by polypeptide chains. The difference among rejections becomes more significant as the feed concentration increases, due to the counterions shielding the membrane charge (Figure 10). All experiments were conducted at the flux that allows the maximum asymptotic rejection.

(27) Kim, K. J.; Stevens, P. V. *J. Membr. Sci.* **1997**, *123*, 303−314.

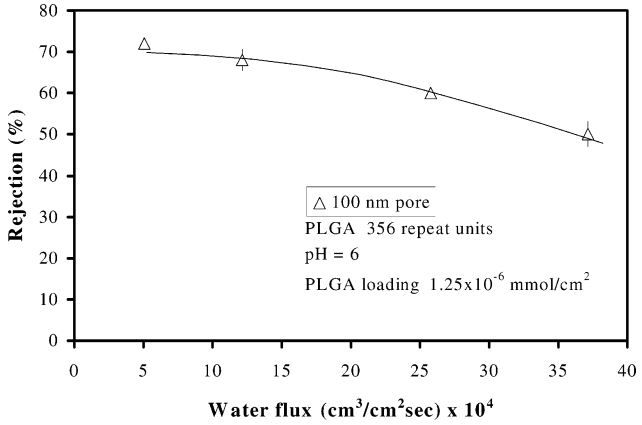

Figure 11. The influence of permeate water flux on 0.5 mM Na_2SO_4 rejection.

The polypeptide chain density is dependent on chain length, due to steric and electrostatic effects. Steric effects lower the chain density because there is a closer packing for shorter chains (116 repeat units) than for longer ones (356 repeat units), and the terminal amine group will be less accessible for the reaction with the aldehyde on the membrane surface. Electrostatic effects are due to the fact that Schiff base reaction must be carried out at high pH (above 9.2, where the terminal amine group on the polypeptide is deprotonated). At this pH the polypeptide is highly charged, which will cause repulsion between chains, lowering the chain density. Higher repulsion is expected between longer chains (more repeating units, all negatively charged). Thus, due to these steric and electrostatic effects, there is a lower chain density and thus lower membrane charge for the 100 nm pore size membrane.

3.5.3. Influence of Flux (Pressure) and Leakage Effects. Polypeptide chains are extended from the surface into the pore. Charged species pass freely through the regions in the pore not covered by the polymer chains. The polypeptide chains can undergo a shear-induced deformation, due to increase in flux, and thus, the size of the central region of the pore not covered by chains increases. This results in higher passage of ions through the membrane without being affected by electrostatics, and as a consequence, the rejection will decrease. Permeability studies on polymer-grafted membranes showed that the thickness of the polymer layer is reduced at high shear rates.[28] The effect of the shear rate (flux) on rejection capability will be more significant for longer chains and low chain densities (as they are more susceptible to deformation). This is the behavior shown by the 100 nm membrane (Figure 11).

In case of the 30 nm membrane, most of the pore is covered by polypeptide chains, leading to high electrostatic interactions between solute and solvent in almost all of the pore volume. The overall effect is that even though some solute escapes through the small gap region, most of solutes are highly rejected in the polypeptide region; also a relatively high chain density will restrict the chain mobility (i.e. chain deformation is much reduced). Thus, in this case, Na_2SO_4 rejection was flux independent for our operating conditions (7.6−9) × 10^{-4} cm^3/cm^2 s at a pressure of 9.7−13.8 bar. This is an intermediate behavior between the first case (100 nm pore size membrane) and the behavior shown by nanofiltration membranes. In nanofiltration, the pore sizes do not exceed a few nanometers and the charge inside the pore is very high, so an increase in flux will cause a higher solute rejection. Mostly, it is the solvent that is transported in these latter membranes.

3.5.4. Simplified Model. The most common approach to describe the ionic transport through the charged membranes is to use the Nernst−Planck equation, which accounts for all three mechanisms: diffusion, convection, and electromigration.

For the 30 nm pore size membrane, after polypeptide immobilization, the spacing between chains (4.6 nm) is comparable with the pore size of a nanofiltration membrane. Therefore, a model (one-dimensional) developed for nanofiltration, based on the Nernst−Planck equation coupled with electroneutrality conditions, was used to describe the transport of ionic species across the membrane. The main equations for this model[29,30] are those for the concentration gradient (eq 3), potential gradient (eq 4), Donnan partition equilibrium at the feed and permeate interfaces (eq 5), as well as the electroneutrality conditions for both the solution phase (eq 6) and inside the membrane (eq 7).

$$\frac{dC_a^m}{dx} = \frac{J_v}{D_{a,p}}(K_{a,c}C_a^m - C_{a,p}) - \left(\frac{z_a C_a^m F}{RT}\right)\left(\frac{d\psi_m}{dx}\right) \quad (3)$$

$$\left(\frac{d\psi_m}{dx}\right) = \frac{\frac{z_a J_v}{D_{a,p}}(K_{a,c}C_c^m - C_{a,p}) + \frac{z_c J_v}{D_{c,p}}(K_{c,c}C_c^m - C_{c,p})}{\frac{F}{RT}(z_a^2 C_a^m + z_c^2 C_c^m)} \quad (4)$$

$$\frac{C_a^m}{C_a} = \left(\frac{|z_a|C_a}{|z_a|C_a^m + |z_m|C_m}\right)^{|z_a|/|z_c|} \quad (5)$$

Electroneutrality in the solution phase, for feed and permeate: $z_a C_a + z_c C_c = 0$ (6)

Electroneutrality in the membrane: $z_a C_a^m + z_c C_c^m = z_m C_m$ (7)

Hindrance factors are considered when the solute moves in a confined space (pore), and $0 < \lambda < 0.4$[31]

For diffusion

$$K_{i,d} = \Phi(1 - 2.1044\lambda + 2.089\lambda^3 - 0.948\lambda^5) \quad (8)$$

$$\Phi = (1 - \lambda)^2 \quad (9)$$

$$D_{i,p} = D_{i,b}K_{i,d} \quad (10)$$

For convection

$$K_{i,c} = \Phi(2 - \Phi)(1 - 0.66\lambda^2 - 0.163\lambda^3) \quad (11)$$

$K_{i,d}$ and $K_{i,c}$ are the diffusive steric hindrance factor and convective coupling, respectively, $D_{i,p}$ and $D_{i,b}$ are the diffusion coefficients in the pore and in bulk solution

(28) Castro, R. P.; Monbouquette, H. G.; Cohen, Y. *J. Membr. Sci.* **2000**, *179*, 207−220.

(29) Peeters, J. M. M.; J. P. Boom; Mulder, M. H. V.; Strathmann, H. *J. Membr. Sci.* **1998**, *145*, 199−209.

(30) Bowen, W. R.; Mukhtar, H. *J. Membr. Sci.* **1996**, *112*, 263−274.

(31) Dean, W. M. *AIChE J.* **1987**, *33*, 1409−1425.

Table 3. Ionic Properties and Hindrance Factors (refs 28 and 31)[a]

species	$D_{i,b} \times 10^9$ (m²/s)	$r_s \times 10^9$ (m)	$\lambda = r_p^*/r_s$	$K_{i,d}$	$K_{i,c}$	$D_{i,p} \times 10^9$ (m²/s)
Na^+	1.333	0.184	0.08	0.7048	0.9722	0.9395
Cl^-	2.031	0.1207	0.052	0.8006	0.9879	1.6261

[a] $r_p^* = 2.3$ nm. $D_{i,b}$ = diffusivity coefficients for species i (anion or cation) in the bulk solution. $D_{i,p}$ = diffusivity coefficients for species i (anion or cation) in the pore. λ = the ratio of the radius of anion or cation to the pore radius. $K_{i,d}$ =diffusive steric hindrance factor. $K_{i,c}$ = convective coupling.

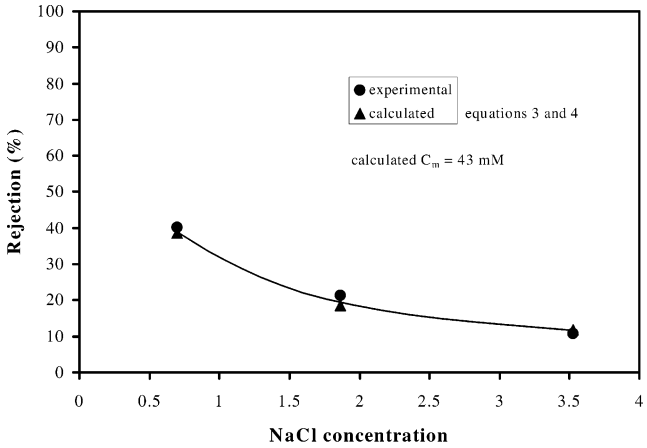

Figure 12. NaCl rejection as a function of feed concentration.

for each of the ions, Φ is steric partition coefficient, and λ is the ratio of the radius of anion or cation to the pore radius (Table 3). All other symbols are defined on a separate list included in this paper.

The Donnan equilibrium equations were used to calculate the concentration of the co-ion (Cl^-) at the feed/membrane ($x = 0$) and membrane/permeate ($x = L$) interfaces. Combining these with electroneutrality conditions and concentration and potential gradient equations, the concentration of the anion (Cl^-) across the membrane thickness (Δx) was numerically calculated. Finally, the observed rejection was calculated using eq 1. In this calculation, the experimental data for NaCl feed concentration, flux, permeate concentration, diffusion coefficients for both ions, and membrane pore size and thickness were used as input parameters, and the calculation was carried out at different C_m values in order to obtain the best fit for experimental/calculated rejection. The rejection vs feed concentration of NaCl is shown in Figure 12. The best fit for calculated/experimental rejection vs feed concentration was obtained at $C_m = 43$ mM.

A membrane charge of ~3−4 mM was recently reported for 36 000 MW PLGA immobilized on a 100 nm diameter silica membrane,[32] and considering the fact that most nanofiltration membranes (1−3 nm diameters) have a charge on the order of $\sim 10^2-10^3$ mM, our value seems reasonable for a membrane with 24.4 nm diameter, immobilized with 17 500 MW PLGA.

It is also possible to estimate the membrane charge based on experimental data; thus, $C_m = m/(N\pi r_p^2 L)$, where m is the amount of PLGA immobilized inside the membrane pores, N and L are number of pores and membrane thickness, respectively, obtained from manufacturer's data, and r_p is the estimated pore radius after gold-coating from SEM images. Assuming straight, cylindrical pores and that the polypeptide chains are uniformly distributed on the membrane area, the calculated charge is 72 mM. Making the same assumption of uniform distribution of polypeptide chains on the total membrane area, but using the pore volume determined from BET, the estimated membrane charge is 13 mM. Thus, the best-fit value of 43 mM lies between these two cases.

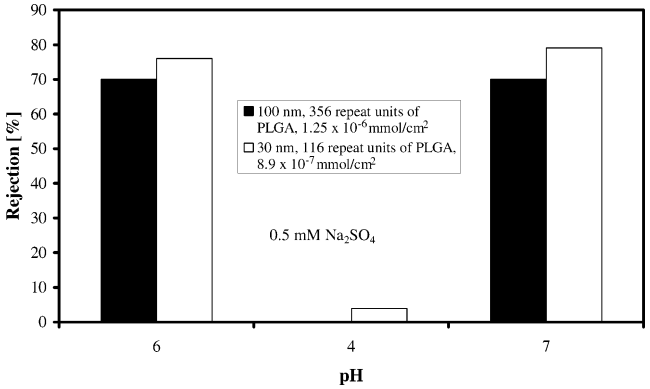

Figure 13. The influence of pH of the feed solution on Na_2SO_4 rejection.

For the 100 nm PCTE−Au−PLGA modified membrane, the size of the pore region not covered by chains was estimated to be ~36.7 nm; this will cause large concentration and potential variations in the radial direction. To realistically predict the solute transport, a two-dimensional model including potential and concentration variation in the radial direction is required. Recently a two-dimensional model for ionic transport across a polypeptide-immobilized 100 nm composite silica−polyethylene membrane was reported.[32]

3.5.5. Influence of Operating pH. As already mentioned, PLGA undergoes conformational changes with pH. At low pH (<4), the polypeptide is present in helix form with the carboxylic acid groups protonated, so the membrane becomes neutral. In contrast, at pH >5.5 the carboxylic acid groups are deprotonated, and the membrane becomes negatively charged. Because the salt rejection is due to electrostatic interactions between the anion and the negative charge on polypeptide chains, it is expected that at pH <4, salt rejection would be very low but high at pH >5.5. This expectation resembles the behavior shown in Figure 13; the rejection decreases from a high value at pH 6−0 at pH 4, and reversibly increases to the original value when the operating pH is >5.5.

3.6. Influence of pH on Permeate Flux. The conformational changes of the polyamino acid will affect not only the rejection capabilities of the PLGA-immobilized membranes but also such conformational changes will cause a change in permeability. The change in polymer brush thickness will affect the porosity, so the flux will decrease at high pH and increase at low pH, all other operating parameters being kept constant. This trend is observed from the results in Table 4.

Under identical operating conditions, for the same feed concentration and pressure, the only variable being pH, it is interesting to observe that, for the 30 nm pore

(32) Hollman, A. M.; Bhattacharyya, D. *J. Membr. Sci.* **2003**, in press.

Table 4. Membrane Permeate Flux Dependence on the pH of the Feed Solution

membrane pore size (nm)	pressure (bar)	flux (cm^3/cm^2 s) × 10^4	
		pH 4	pH 6
30	7	5.3	4.8
100	0.3	15.8	10.7

size membrane (24.4 nm after gold coating) functionalized with 17 500 MW PLGA, only a 12% reduction in flux was observed by changing the pH from 4 to 6. We attributed this to the fact that helix−coil transitions are hindered due to a very confined environment inside the pore. For comparison, for a 200 nm pore size PCTE membrane immobilized with 17 400 MW PLGA the flux reduction was reported to be ∼55%.[33]

For the 100 nm pore size membrane gold-coated and functionalized with 54 000 MW PLGA, changing the pH from 6 to 4 reduced the flux over 30%. In addition to the pore size, an important role in flux decrease is played by the polypeptide chain length, with longer chains showing less mobility during helix−coil transitions,[9] as well as by surface chain density, with the flux from pH 4 to 6 decreasing with increasing chain density.[9] Overall, the ratio of pore size/chain length governs the changes in permeability in response to pH variations.

4. Conclusions

A new method of polypeptide immobilization, with a high chain density, on a membrane with a known structure was successfully accomplished. Our investigation has shown that membrane performance, evaluated in terms of both permeability and retention capabilities, can be reversibly modulated by changing the pH. Since the membrane has a defined structure, its rejection capacity can be improved by choosing the appropriate ratio of polypeptide chain length/membrane pore size. To show a high ionic rejection, the degree of attachment of polypeptide on the membrane has to be increased. This can be achieved by decreasing the electrostatic repulsion between chains, either by performing the immobilization in an aqueous/ethanol mixture or in an aqueous solution under increased ionic strength. The polypeptide chains covalently attached to the membrane can constitute a solid backbone for deposition of ultrathin self-assembled monolayers of polyanions and polycations. Our membrane modification procedure may provide an alternative route for producing stimuli-responsive materials. Because biological molecules have many amine residues, Schiff-base reaction of various biomolecules with application in separations, catalysis, and sensing may be accomplished using the membrane system described here.

Acknowledgment. This work was partially supported by a U.S. EPA STAR grant.

List of Symbols

C_a = anion concentration in the bulk solution (mmol/L)
C_a^m = anion concentration in the membrane (mmol/L)
$C_{a,p}$ = anion concentration in the permeate (mmol/L)
C_c = cation concentration in the bulk solution (mmol/L)
C_c^m = cation concentration in the membrane (mmol/L)
$C_{c,p}$ = cation concentration in the permeate (mmol/L)
C_m = effective membrane charge (mmol/L)
$D_{a,b}$ = bulk anion diffusivity (m^2/s)
$D_{a,p}$ = hindered anion diffusivity (m^2/s)
$D_{c,b}$ = bulk cation diffusivity (m^2/s)
$D_{c,p}$ = hindered cation diffusivity (m^2/s)
$D_{i,b}$ = diffusivity coefficients for species *i* (anion or cation) in the bulk solution (m^2/s)
$D_{i,p}$ = diffusivity coefficients for species *i* (anion or cation) in the pore (m^2/s)
F = Faraday constant (C/mol)
J_v = solvent volume flux (based on membrane area) (m/s)
$K_{i,d}$ = diffusive steric hindrance factor for species *i*
$K_{i,c}$ = convective coupling for species *i*
N = number of pores
R = gas constant (J/mol K)
T = absolute temperature (K)
z_a = anion charge (−1)
z_c = cation charge (+1)
z_m = membrane charge (−1)
Φ = steric partition coefficient
λ = the ratio of the radius of the anion or cation to the pore radius
Δx = membrane thickness (m)
ψ_m = electric potential in the membrane (V)
σ = pore density (pores/cm^2)
θ = membrane porosity (%)

Chemical Abbreviations

PLGA = poly-L-glutamic acid
PVP = poly(vinylpyrrolidone)
MPD = 3-mercapto-1,2-propanediol
DTNB = 5,5′-dithiobis(2-nitrobenzoic acid)
PEG = poly(ethylene glycol)

CM035323J

(33) Ito, Y. *Nanotechnology* **1998**, *9*, 205−207.